RSC Advances

COMMUNICATION

View Article Online
View Journal | View Issue

Cite this: *RSC Adv.*, 2016, **6**, 20453

Received 22nd December 2015
Accepted 10th February 2016

DOI: 10.1039/c5ra27403f

www.rsc.org/advances

Time-resolved XAS/MS/Raman monitoring of mutual copper self-reduction and ethanol dehydrogenation reactions†

Wellington H. Cassinelli,*[a] Leandro Martins,[a] Marina Magnani,[a] Sandra H. Pulcinelli,[a] Valérie Briois[b] and Celso V. Santilli[a]

Selective ethanol dehydrogenation using a Cu/Al_2O_3 catalyst was investigated by time-resolved XAS/MS/Raman techniques. On-line monitoring of the reaction products revealed that formation of H_2 and acetaldehyde occurs over intermediate Cu^+ species self-reduced upon reaction and the selectivity to ethyl acetate results in coupling of acetyl and ethoxy species over mixed Cu°/Cu^+ active sites.

In recent years, the need to reduce dependency on fossil fuels and decrease emissions of greenhouse gases (GHG) has motivated the use of clean and renewable energy sources inducing large increases in the production of biofuels such as biodiesel, biogas, and bioethanol. The advances in research concerning first and second generation ethanol technologies have led to a significant increase in global ethanol production, reaching 86 billion liters in 2011.[1] The use of ethanol in motor vehicles, alone or in mixtures with gasoline, can decrease net GHG emissions by 90%, compared to an equivalent amount of gasoline.[2] This renewable energy source can also be used in the so-called ethanol dehydrogenation reaction (EDR) for the green production of chemicals such as H_2, acetaldehyde, ethyl acetate, and *n*-butanol, amongst others. Since these compounds are normally obtained from fossil fuel sources, their production from bioethanol, for instance produced from sugarcane, offers a way of overcoming the shortage of fossil fuel sources as well as reducing emissions of GHG.

Supported copper is the most widely used catalyst for alcohol dehydrogenation, and its selectivity towards different products changes according to catalytic features such as the acid–basic characteristics of the support,[3,4] Cu loading, metal dispersion, and residence time.[5,6] However, there is a lack of conclusive information about the oxidation state of the active Cu species in the EDR. Some studies have suggested that metallic copper is the active species,[7,8] while others have found that the presence of Cu^+ species in association with Cu° can optimize the activity and selectivity.[5,9,10]

In the present work, it is shown that the activation process can be integrated with the reductive atmosphere provided by the EDR stream, which is important from the economic perspective. Clear correlation between the oxidation state of the active copper, the catalytic performance, and the selectivity of the catalyst was revealed from monitoring of the copper species by time-resolved XAS combined with determination of the EDR products using on-stream mass spectrometry and Raman spectroscopy measurements.

The copper-based catalyst was composed of well-dispersed 20 wt% of copper (20Cu/Al) supported on macro–mesoporous alumina.[10] The catalyst was synthesized by wetness impregnation of calcined porous Al_2O_3 (S_{BET} = 577 m^2 g^{-1}) using an aqueous copper nitrate solution. After impregnation, the sample was calcined in a conventional muffle furnace at 500 °C for 2 h. Transmission electron microscopy (TEM) characterization of the as-prepared catalyst was carried out at the Brazilian Nanotechnology National Laboratory (LNNano), using a JEOL JEM 3010 microscope operated at 300 kV (1.7 Å resolution). The sample was prepared by dropping an isopropanolic suspension of the catalyst onto amorphous carbon films supported on nickel grids.

Fig. 1(a) shows a TEM image of the calcined 20Cu/Al sample, revealing that the copper species were well dispersed on the Al_2O_3 surface. The pore size distributions determined by means of N_2 adsorption–desorption isotherms (Fig. S1, ESI†) showed that the porous Al_2O_3 used as support had a mesopore size distribution centered at 7.8 nm that could limit the size of the unreduced copper, which was mainly present as CuO particles in the as-synthesized samples. The bright-field and dark-field images (Fig. 1(a) and (b)) revealed an average particle size of 2.4 ± 1.1 nm, which was smaller than the average mesopore size of the Al_2O_3 support. The electron diffraction pattern measured

[a]*Instituto de Química, Universidade Estadual Paulista – UNESP, Rua Professor Francisco Degni, 55, 14800-060, Araraquara, SP, Brazil. E-mail: cassinelli@iq.unesp.br; Fax: +55-16-33222308; Tel: +55-16-33019758*

[b]*Synchrotron SOLEIL, L'Orme des Merisiers, BP48, Saint Aubin, 91192 Gif-sur Yvette, France*

† Electronic supplementary information (ESI) available. See DOI: 10.1039/c5ra27403f

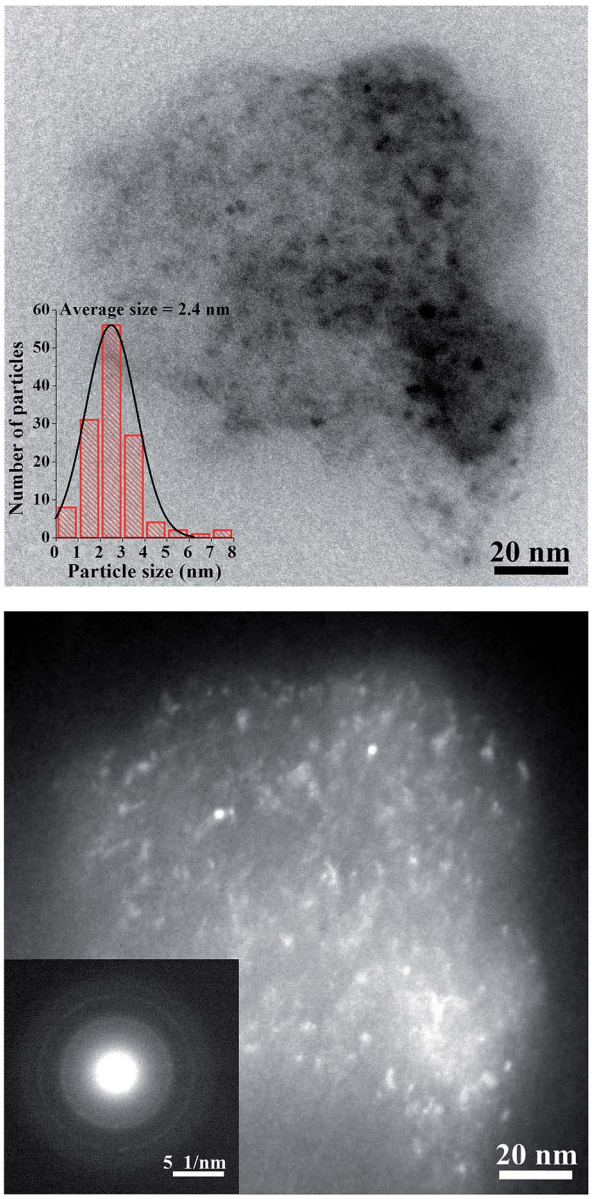

Fig. 1 TEM images of the 20Cu/Al catalyst. (a) Bright-field and particle size distribution, and (b) dark-field and electron diffraction.

in the same region shown in Fig. 1(a) and (b) indicated a low degree of crystallization, reflecting a distribution of Cu species with no long-range order on the alumina support. Despite the high loading of copper used for catalyst preparation, the absence of large CuO agglomerates in the TEM images clearly evidences the capacity of the porous Al_2O_3 with high surface area to disperse a high amount of oxidic Cu^{2+} species, with monolayer or sub-monolayer coverage. Previous work[11] found that surface saturation of Al_2O_3 by copper was achieved with approximately 4–5 wt% of Cu per 100 m^2 g^{-1} of γ-Al_2O_3. Here, the high surface area of the support (S_{BET} = 577 m^2 g^{-1}) was responsible for the formation of an incomplete monolayer of copper on the surface of the alumina, even with such a high Cu loading (20 wt%). This feature is a fundamental prerequisite from the standpoint of catalytic performance, because a greater quantity of well-dispersed copper species increases the number of available active sites.

In order to demonstrate the feasibility of self-activation of the as-prepared oxidic copper catalyst, time-resolved *operando* monitoring of the effluents using XAS, mass spectrometry, and Raman analysis was performed during the EDR, using a dedicated cell connected to the gas feeding system installed at the SAMBA beamline of the SOLEIL synchrotron.[12] Time-resolved spectra were collected *in situ* using a Quick-XAS monochromator equipped with a Si(111) channel-cut crystal whose oscillatory movement was set to acquire one spectrum every 0.5 s.[13] The effluent gas at the reactor outlet was monitored on-line using mass spectrometry (Cirrus system, MKS) and Raman spectroscopy (RXN1 system equipped with a sensitive Air-Head™ probe, Kaiser Optical Systems, Inc.). Table 1 (ESI†) gives the mass fragments used for product monitoring, together with the Raman band positions of gaseous products of interest. Evolution of Raman bands regarding ethanol consumption (2865 cm^{-1}) and H_2 formation (585 cm^{-1}) are also illustrated in the Fig. S2.† The reaction was performed using isothermal steps of 50 °C in the range from 200 to 400 °C, with 45 min at each temperature, using 15.2 mg of 20 wt% copper catalyst diluted in boron nitride (mass dilution of about 45%). The heating rate for changing the isothermal reaction temperature was set to 10 °C min^{-1}. Ethanol was introduced to the catalytic reactor by passing a flow of helium (at 40 mL min^{-1}) through a saturator containing liquid ethanol immersed in a temperature-controlled bath at 43 °C. The XANES data analysis was performed using Athena[14] software and copper speciation was obtained by linear combination fits (LCF). The XANES spectra of the pure copper reference species (in the Cu^{2+}, Cu^{+}, and Cu° oxidation states) employed in the LCF were processed using a multivariate curve resolution with alternating least squares procedure (MCR-ALS). The chemometric method was described fully in a previous paper that focused on the copper speciation resulting from temperature programmed reduction (TPR) of the same Cu-based catalysts.[15]

Fig. 2(a) shows the Cu K-edge normalized XANES and Fourier transforms (FT) of the EXAFS spectra (not corrected for phase shift) obtained for the calcined 20Cu/Al catalyst during the EDR. Each spectrum in Fig. 2(a) was collected after 45 min of reaction at a given isothermal temperature. For comparison, the data for the sample collected before the reaction at 200 °C are also displayed. The XANES spectrum presented an intense white line characteristic of divalent oxidic Cu^{2+} species. It can be seen from Fig. 2(a) that the intensity of the white line did not change during the first isothermal step at 200 °C. However, there were clear decreases of the white line during the second and third isothermal temperature steps at 250 and 300 °C, respectively (Fig. 2(b)). At the end of these isothermal steps, there was a decrease in the intensity of the first FT peak located between 1.0 and 2.0 Å, corresponding to the Cu–O contribution. There was also an increase in the intensity of the peak located between 2.2 and 2.7 Å, corresponding to the Cu–Cu contribution of Cu° species. There was a progressive decrease of the white line and changes in the intensity of the FT peaks during the 45 min of

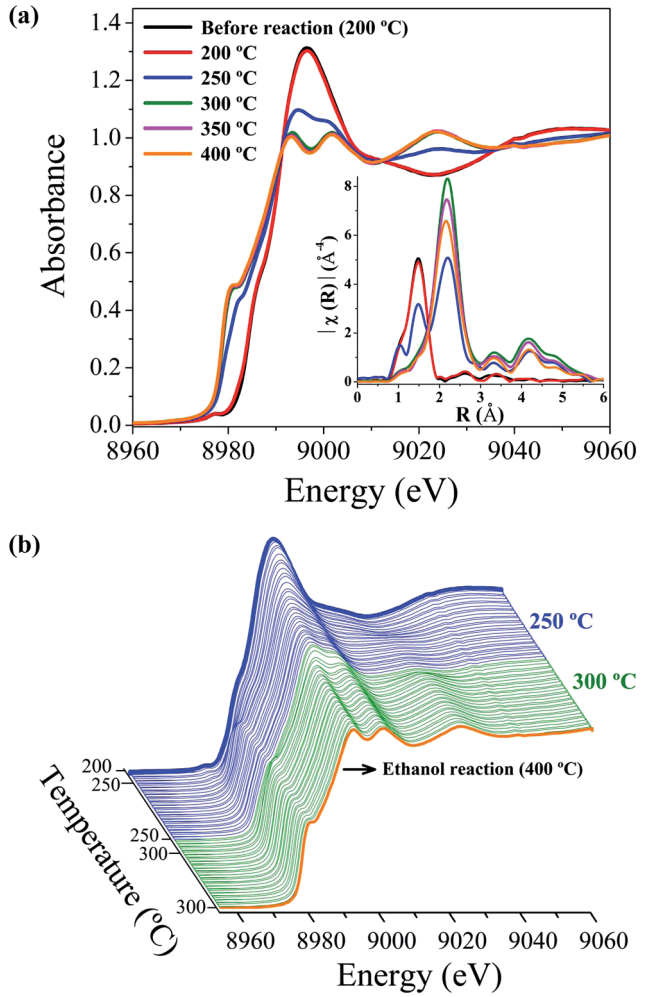

Fig. 2 (a) Cu K-edge XANES and Fourier transformed EXAFS spectra of the 20Cu/Al catalyst collected during the ethanol dehydrogenation reaction from 200 to 400 °C. (b) Quick-XANES spectra recorded during the ethanol dehydrogenation reaction from 200 to 300 °C.

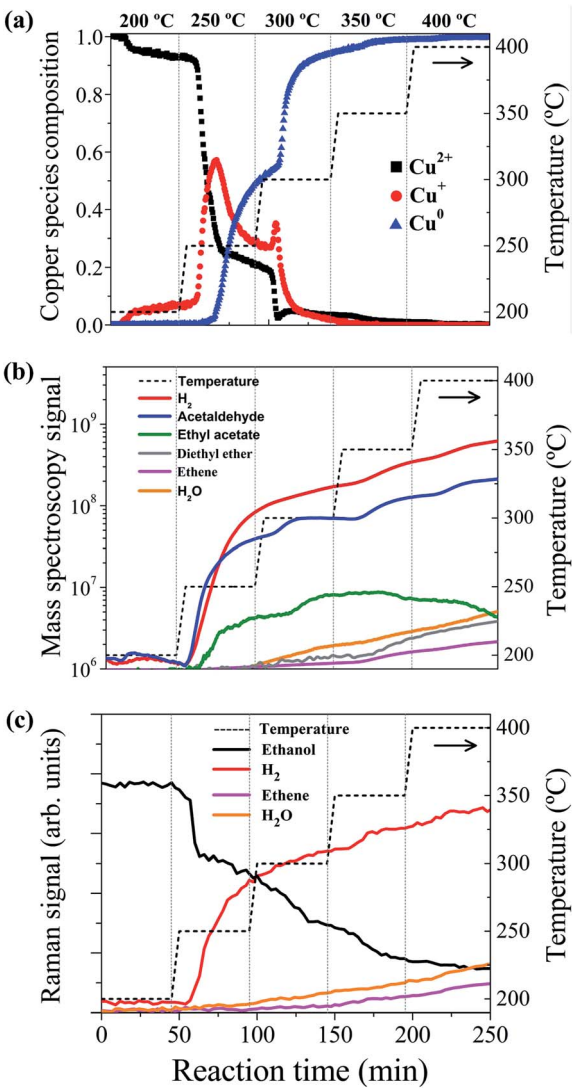

Fig. 3 (a) Copper speciation during the ethanol dehydrogenation reaction obtained from time-resolved Cu K-edge XANES measurements; (b) and (c) distribution of products with ethanol on-stream obtained using mass spectrometry and Raman spectroscopy, respectively.

isothermal treatment at 250 °C with ethanol on-stream. During the third isothermal step at 300 °C, copper was almost completely reduced; full reduction was achieved at 350 °C, as evidenced by the XANES fingerprints shown in Fig. 2(a). The decrease in intensity of the Cu–Cu contribution to the FT during heating from 300 to 400 °C was mainly related to the increase of Debye–Waller factors, due to the increase of the thermal vibrations.

Fig. 3(a)–(c) show the Cu speciation obtained by LCF analysis of the Cu K-edge XANES and reaction effluent monitoring data acquired during the ethanol dehydrogenation. The speciation indicated that at the time that mainly Cu^{2+} species were present in the reaction at 200 °C, there was no substantial formation of products with ethanol on-stream. The increase in the temperature from 200 to 250 °C promoted self-activation of the copper. At this stage, there was an abrupt consumption of ethanol (Fig. 3(c)), and the formation of H_2 and acetaldehyde (Fig. 3(b) and (c)) was identified when Cu^+ species started to be formed by partial reduction of Cu^{2+} ($Cu^{2+} \rightarrow Cu^+$). Similar abrupt consumption of ethanol was not observed for reduced 20Cu/Al catalyst in the ethanol dehydrogenation reaction (Fig. S3†). After reaching a maximum value of about 60%, a decrease in the amount of Cu^+, together with a concomitant increase of the Cu° species. As there was no substantial change in the Cu^{2+} concentration during this stage, the formation of Cu° was related to a second reduction process involving monovalent copper ($Cu^+ \rightarrow Cu^\circ$). This second reduction stage was accompanied by a two-fold decrease in the conversion of ethanol and production of acetaldehyde. The selectivity towards H_2 continued to increase, despite a slight slowdown of the formation rate, while the ethyl acetate concentration started to increase due to the dehydrogenation of acetaldehyde over the mixture of Cu°/Cu^+ active sites. It is noteworthy that there was consumption of H_2 during the second reduction stage, so the

hydrogen concentration observed did not reflect the full quantity of H_2 formed during this stage. The increase of the reactor temperature to 300 °C promoted a new abrupt increase in the Cu^+ concentration, resulting from the fast reduction of Cu^{2+}. This speciation change was accompanied by an additional increase in acetaldehyde production. After total reduction of the Cu species with further increase of temperature ($T > 300$ °C), the increment in ethanol conversion achieved at each temperature was smaller than the values observed at lower temperatures. Above 350 °C, the selectivity towards ethyl acetate decreased, and there were increases in the concentrations of products such as ethene, diethyl ether, and water, resulting from ethanol dehydration reactions (Fig. 3(b)).

It has been proposed that Cu° is able to activate the O–H bond of ethanol adsorbed on catalytic surfaces.[3,16] However, recent studies have shown that an optimal Cu°/Cu^+ ratio can also promote faster ethanol dehydrogenation on Cu catalysts supported on Al_2O_3 and ZrO_2.[5,10,17] In the present case, the *operando* quick-XAS/MS/Raman results revealed no significant ethanol activation in the presence of supported Cu^{2+} species at 200 °C. The onset of acetaldehyde formation was evident at higher temperatures, when the concentration of Cu^+ increased considerably as a result of the reduction of Cu^{2+} species, first after heating from 200 to 250 °C, and then from 250 to 300 °C. The maximum rate of acetaldehyde formation, as shown by the derivative curve (Fig. S4†), occurred without any substantial presence of reduced Cu° species, while the maximum rate of H_2 production was observed when the quantity of intermediate Cu^+ species reached a maximum. These results, together with the decrease in the acetaldehyde formation rate with further reduction of Cu^+ to Cu° at the end of the isothermal treatment at 250 °C caused by the increase in the ethyl acetate formation rate, provided strong evidence that Cu^+ was more active than Cu° in promoting the first ethanol dehydrogenation towards acetaldehyde and H_2. During the copper activation, it was possible to identify the most active species for acetaldehyde formation, because formation of the Cu^+ intermediate was associated with the self-production of H_2 caused by the dehydrogenation of ethanol to acetaldehyde. The amount of H_2 formed in this process was at a concentration suitable for sustaining the Cu^+ intermediate throughout the treatment of the 20 wt% Cu catalyst at 250 °C. In previous work investigating the activation of Cu under an H_2/He atmosphere (heating from 50 to 250 °C, with isothermal treatment at 250 °C for 0.5 h), using Cu-based catalysts prepared from the same porous alumina support, it was found that the lifetime of the Cu^+ species at 250 °C was shorter than observed here.[10] Although a similar maximum value of about 60% of intermediate Cu^+ species was achieved when the temperature reached 250 °C, the second reduction stage leading to Cu° occurred during the same period. In our recent work,[10] it was found that for Cu loadings in the range from 5 to 20 wt% in catalysts prepared on the Al_2O_3 support, the intermediate Cu^+ species formed by classical TPR treatment became stabilized as the loading was decreased. In this case, the onset temperature of the $Cu^{2+} \rightarrow Cu^+$ reduction was significantly lower than the temperature leading to the formation of Cu° species. The stability of the Cu^+ intermediate on the porous alumina was proposed to be related to the isolated Cu ions bound to the vacant Al^{3+} sites, as well as to the large diffusion distances between Cu^+ ions adsorbed in a diluted sub-monolayer, which increased as the Cu loading decreased.

The development of $Cu^+ \rightarrow$ Cu° reduction from 250 °C resulted in an increase in the concentration of Cu°. During this stage, the ethyl acetate formation rate started to increase due to interaction between the adsorbed ethoxy and acetyl species, leading to a decrease in the acetaldehyde formation rate (Fig. S4†). The increase in the ethyl acetate yield was in agreement with previous findings,[9] where the presence of Cu° together with isolated partially oxidized Cu^+ was able to activate the C–H bond in the adsorbed CH_3CH_2O–Cu^+ and promote the formation of ethyl acetate by coupling with the acetyl (CH_3CO) fragment.[18] The present results (Fig. 3) showed that there was no further increase in the concentration of ethyl acetate after the full reduction of copper species achieved by increasing the reaction temperature to 350 °C. This confirms the key role of the Cu^+/Cu° balance in the production of ethyl acetate from ethanol dehydrogenation. Similar results were reported by Inui *et al.*,[19] with the coupling of ethanol with acetaldehyde for ethyl acetate formation occurring over a mixed metal-oxides surface (Cu^+ and Cu°), but not over a Cu° surface.

In summary, we have demonstrated a correlation between catalytic performance in the ethanol dehydrogenation reaction and the most active oxidation state of copper species supported on porous alumina. The combination of time-resolved XAS/MS/Raman techniques revealed an abrupt consumption of ethanol and a pronounced increase of formation of H_2 and acetaldehyde as Cu^+ started to be formed ($Cu^{2+} \rightarrow Cu^+$) and reached its maximum concentration. During the development of the second reduction stage ($Cu^+ \rightarrow$ Cu°), the consumption of ethanol, and the formation of H_2 and acetaldehyde, were not maintained at elevated rates, because ethyl acetate production started. From these results, it can be concluded that Cu^+ is the most active species for promotion of the first ethanol dehydrogenation. On the other hand, the combined presence of Cu^+/Cu° species results in an increase in the formation of ethyl acetate by the coupling of acetyl (CH_3CO) and ethoxy (CH_3CH_2O) fragments. It should be noted that the methodology used in this work, based on the combination of time-resolved XAS/MS/Raman techniques, is not only suitable for studying the ethanol dehydrogenation process, but also offers a valuable means of understanding active species in many other industrially relevant processes involving the use of supported catalysts.

Acknowledgements

This work was supported by the Brazilian agencies: CAPES, CNPq, and FAPESP (project numbers 07/53073-4, 2010/01449-3, 2013/50023-7, and 2013/05346-2) and by a FAPESP/CNRS bilateral cooperation program. The authors are grateful to LNNano (CNPEN) for the TEM images, and to SOLEIL Synchrotron for providing beam time at the SAMBA beamline.

Notes and references

1 S. Kumar, P. Shrestha and P. Abdul Salam, *Renewable Sustainable Energy Rev.*, 2013, **26**, 822–836.
2 G. R. Timilsina and A. Shrestha, *Energy*, 2011, **36**, 2055–2069.
3 P. C. Zonetti, J. Celnik, S. Letichevsky, A. B. Gaspar and L. G. Appel, *J. Mol. Catal. A: Chem.*, 2011, **334**, 29–34.
4 J. M. Vohs, *Chem. Rev.*, 2013, **113**, 4136–4163.
5 I. C. Freitas, S. Damyanova, D. C. Oliveira, C. M. P. Marques and J. M. C. Bueno, *J. Mol. Catal. A: Chem.*, 2014, **381**, 26–37.
6 K. Inui, T. Kurabayashi and S. Sato, *J. Catal.*, 2002, **212**, 207–215.
7 N. Iwasa and N. Takezawa, *Bull. Chem. Soc. Jpn.*, 1991, **64**, 2619–2623.
8 S. W. Colley, J. Tabatabaei, K. C. Waugh and M. A. Wood, *J. Catal.*, 2005, **236**, 21–33.
9 A. G. Sato, D. P. Volanti, I. C. de Freitas, E. Longo and J. M. C. Bueno, *Catal. Commun.*, 2012, **26**, 122–126.
10 W. H. Cassinelli, L. Martins, A. R. Passos, S. H. Pulcinelli, A. Rochet, V. Briois and C. V. Santilli, *ChemCatChem*, 2015, **7**, 1668–1677.
11 R. M. Friedman, J. J. Freeman and F. W. Lytle, *J. Catal.*, 1978, **55**, 10–28.
12 C. La Fontaine, L. Barthe, A. Rochet and V. Briois, *Catal. Today*, 2013, **205**, 148–158.
13 E. Fonda, A. Rochet, M. Ribbens, L. Barthe, S. Belin and V. Briois, *J. Synchrotron Radiat.*, 2012, **19**, 417–424.
14 B. Ravel and M. Newville, *J. Synchrotron Radiat.*, 2005, **12**, 537–541.
15 W. H. Cassinelli, L. Martins, A. R. Passos, S. H. Pulcinelli, C. V. Santilli, A. Rochet and V. Briois, *Catal. Today*, 2014, **229**, 114–122.
16 D. Gao, Y. Feng, H. Yin, A. Wang and T. Jiang, *Chem. Eng. J.*, 2013, **233**, 349–359.
17 A. G. Sato, D. P. Volanti, D. M. Meira, S. Damyanova, E. Longo and J. M. C. Bueno, *J. Catal.*, 2013, **307**, 1–17.
18 J. C. Kenvin and M. G. White, *J. Catal.*, 1992, **135**, 81–91.
19 K. Inui, T. Kurabayashi, S. Sato and N. Ichikawa, *J. Mol. Catal. A: Chem.*, 2004, **216**, 147–156.